THE EFFECT OF DEVELOPMENT ON SPATIAL PATTERN SEPARATION IN THE HIPPOCAMPUS AS QUANTIFIED BY THE *HOMER1A* IMMEDIATE-EARLY GENE

JEANNE YAN XIE
Bachelor of Science, Cornell University, 2009

A Thesis
Submitted to the School of Graduate Studies
of the University of Lethbridge
in Partial Fulfillment of the
Requirements for the Degree

MASTER OF SCIENCE

Department of Neuroscience
University of Lethbridge
LETHBRIDGE, ALBERTA, CANADA

ABSTRACT

This study sought to determine whether the DG, CA3, and CA1 regions contain uniformly excitable populations and test the hypothesis that rapid addition of new, more excitable, granule cells in prepubescence results in a low activation probability (P_1) in the DG. The immediate-early gene *Homer1a* was used as a neural activity marker to quantify activation in juvenile (P28) and adult (~5 mo) rats during track running. The main finding was that P_1 in juveniles was substantially lower not only the DG, but also CA3 and CA1. The P_1 for a DG granule cell was close to 0 in juveniles, versus 0.58 in adults. The low P_1 in juveniles indicates that sparse, but non-overlapping, subpopulations participate in encoding events. Since sparse, orthogonal coding enhances a network's ability to decorrelate input patterns (Marr, 1971; McNaughton & Morris, 1987), the findings suggest that juveniles likely possess greatly enhanced pattern separation ability.

ACKNOWLEDGMENTS

I owe many thanks to my supervisor, Dr. Bruce McNaughton. It has been truly rewarding and inspiring to have an advisor so willing to share the vast depths of his knowledge on not only the brain, but also how to think critically in science. I am grateful for the discussion and helpful comments from my committee members, Dr. Rob Sutherland and Dr. David Euston, and my committee chair Dr. Andy Iwaniuk.

I am greatly indebted to those who spent many hours in the technical trenches in helping this project along: Charlotte Alme, Aubrey Demchuk, Val Lapointe, Vivek Trivedi, Melinda Wang, Geoff Minors, Karen Dow-Cazal, and Amanda Mauthe-Kaddoura - you are all champions.

The continuous support and encouragement from my colleagues, family, and friends were profoundly important throughout this journey. For the numerous, often spontaneous, exchanges of ideas and expertise that took place at the CCBN, I am particularly grateful towards Ben Clark, Robin Keeley, and Aaron Wilber for being so generous with their time. I thank my mom and dad, whose insightful words were often accompanied by reluctant, but necessary, introspection. I am tremendously thankful for being able to draw upon such a richly diverse group of friends. In particular, I thank Wing Witharana and Sutherland Dube for caring fiercely for my spirit; and Daniela Schwindel and Zaneta Navratilova for always giving me a belay.

TABLE OF CONTENTS

LIST OF TABLES

LIST OF FIGURES

LIST OF ABBREVIATIONS

CA	*cornu ammonis*
DAPI	4'-6-diamidino-2-phenylindole
DG	Dentate gyrus
FISH	Fluorescence *in situ* hybridization
FITC	Fluorescein isothiocyanate
GC	Granule cell
H1a	*Homer1a*
HPC	Hippocampus
HRP	Horseradish peroxidase
HV	Hight voltage
IEG	Immediate-early gene
INF	Intranuclear foci
LUT	Look-up table
MECS	Maximal electroconvulsive shock
PBS	Phosphate buffered saline
PFA	Paraformaldehyde
UTR	Untranslated region

CHAPTER 1 INTRODUCTION

In a given environment, some hippocampal cells are active while others are silent. The mechanism by which certain cells are allocated to space is not entirely understood. In the absence of a clear model, the default hypothesis of random sample with replacement has often been assumed. This model assumes that all cells are uniformly excitable and, thus, each neuron has equal probability of being active in a given environment (P_1). When this uniform population encounters two different uncorrelated environments, random sample with replacement dictates that statistically independent subpopulations are active in each environment and that the probability of overlap between the subpopulations is the square of P_1. This study sought to determine whether the DG, CA3, and CA1 hippocampal populations indeed contain uniformly excitable cells by comparing empirically derived P_1 values with those predicted by random sample with replacement. Another goal was to test the hypothesis that the rapid addition of new, presumably more excitable, granule cells to the hippocampus in prepubescence results in activation probabilities that are lower but more uniform across the population, possibly leading to enhanced neural representations of different spaces.

A. Different spatial encoding dynamics in hippocampal populations

Some data from ensemble recordings and immediate-early gene markers for neural activity appear to be consistent with random sample with replacement spatial encoding dynamics, while other data suggest that cells are assigned to space in a nonrandom fashion. Random sampling within a neural population would cause

statistically independent groups of cells to be active in each location, thus resulting in global remapping of place field locations. Ensemble recordings in the hippocampus, indeed, show uncorrelated place field maps when the animal moves between two recognizably different environments (J. K. Leutgeb, Leutgeb, Moser, & Moser, 2007; S. Leutgeb et al., 2005; Muller & Kubie, 1987). Additionally, at least some studies using the neural activity marker *Arc* gene show that, compared to successive visits to a single environment (A/A condition), two different environments (A/B condition) induce activity across subsets of neurons in a manner consistent with random sample with replacement predictions (Guzowski, McNaughton, Barnes, & Worley, 1999). For instance, given that approximately 40% of CA1 neurons are active in an environment, two environments of the same size activate three subsets of neurons comprised of two non-overlapping neural subpopulations of similar size (22% and 23%) and a third subpopulation of neurons active in both environments (16%) (Guzowski et al., 1999). The resulting empirical P_1^2 value is 0.16, as predicted by random sampling within the population.

Some whole-cell current clamp recordings in the dorsal CA1 region of free moving rats suggest, conversely, that the identity of cells with spatially tuned firing in a novel environment is not due random selection. Differences between future place cells and silent cells are observable in the first spatial exploration: future place cells show lower action potential thresholds and spatially selective subthreshold fields, versus the flat fields in silent cells (Epsztein, Brecht, & Lee, 2011). Pre-exploration current injection in the anesthetized animal, furthermore, reveal a distinct tendency of future place cells to exhibit a bursting response that is absent in silent cells (Epsztein et al., 2011). Some

hippocampal neurons, thus, appear to be 'preselected' to become place cells even before sensory input of the novel environment. Contrary to the default assumption of a uniform distribution of activation probability in the hippocampus, these data seem to suggest a skewed distribution of excitability, in which some cells are much more likely to fire than others in a spatial context.

B. Distribution of excitability in the DG granule cell population

Within a uniformly excitable population, high sparsity results in very little overlap between the populations that encode for uncorrelated environments. This pattern separation mechanism theoretically would enhance a network's ability to orthogonalize representations for similar input patterns (Marr, 1971; McNaughton & Morris, 1987). Coding in the dentate gyrus (DG) cell population is highly sparse, with around 2-5% activation in a behavioral context (Chawla et al., 2005; Jung & McNaughton, 1993); therefore, the DG is hypothesized to mediate pattern separation by decorrelating inputs into CA3 (Guzowski, Knierim, & Moser, 2004; J. K. Leutgeb et al., 2007). This hypothesis, however, is predicated on the assumption of equal probabilities of activation in the DG population.

Recent electrophysiological and IEG marker data, however, suggest that the DG granule cell (GC) population is not uniformly excitable; instead, some cells are much more likely than others to exhibit activity in a given environment (Alme et al., 2010; Chawla et al., 2005). In the Alme et al. study, animals consecutively explored a single environment four times or four unique environments. Random sample with replacement

predicts that, with high sparsity typical of the DG, the number of active neurons will increase as a product of the number of environments; i.e. if X_1 is the number of neurons active in one environment (Figure 1.1A), the expected number of neurons active from n uncorrelated environments would be close to nX_1 (Figure 1.1B). The study found that the total number of neurons activated in the multiple environment condition (X_n) relative to the single environment condition (X_1) was much lower than the predicted estimate (1.33 versus 3.94) (Figure 1.1C). This X_n/X_1 value corresponded to an actual P_1 of 0.6, which was determined using an estimator method that does not assume uniform excitability across all anatomically identifiable cells. Electrophysiology data in the same study showed that the mean probability of a granule cell expressing at least one place field in an environment was 0.69, similar to the IEG based value. In all, the data seem to indicate that the DG cell population is characterized by a highly skewed distribution of excitability, and the random sample with replacement model does not predict the manner in which these cells are allotted to space.

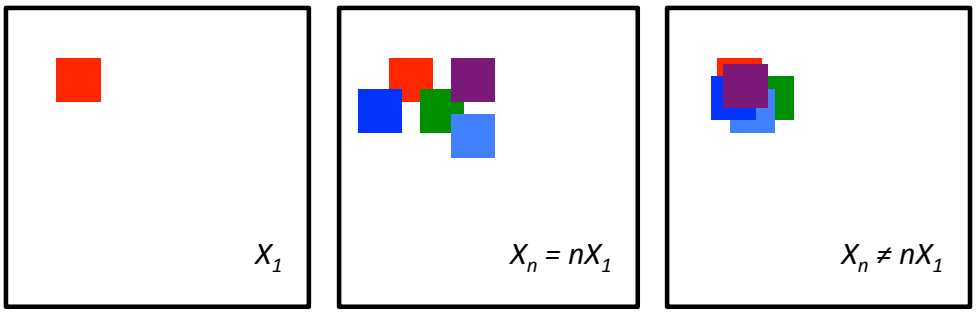

Figure 1.1 Schematic representation of the active DG subpopulation. A: the colored box represents the active subpopulation in one environment (X_1); B: the predicted active subpopulation in n environments based on random sampling (X_n); and C: the empirical active subpopulation in n environments.

In light of the foregoing findings, an alternative 'early retirement' hypothesis was proposed, which suggested that after an initial period of enhanced excitability, the vast majority of GCs enter into a state of hypo-excitability and rarely, if ever, spike in a behavioral context (2010). The hypothesis posits that the excitable subpopulation, only about 5% of all GCs, participates in the encoding of many events, so that activation within this limited population is non-sparse. A major goal of the study described here was to confirm the Alme et al. findings that substantial overlap exists in the encoding DG granule cell populations across multiple environments.

C. Influence of age on population activity in the DG

The 'early retirement' theory further proposes that the identity of the encoding neurons corresponds to the continually changing pool of newborn neurons generated from adult neurogenesis (Altman, 1963; Altman & Das, 1965). The idea that newborn neurons make up the majority of the active GCs is compatible with what is known about adult neurogenesis and the physiological properties of newborn neurons. First, the proportion of active GCs in a behavioral context is very similar to the proportion of adult-generated newborn neurons in the granule cell layer. In young adult rats, the proportion of cells born per month is approximately 6% of the granule cell population (Cameron & McKay, 2001); however, many newly generated cells normally die between the first two weeks of cell age (Gould, Beylin, Tanapat, Reeves, & Shors, 1999), so that the proportion of newborn neurons contributing to hippocampal function is likely closer to the 3-5% of GCs that participate in behavior. Second, physiological changes in adult-generated

neurons during maturation parallel those proposed by the 'early retirement' theory. Between 1-2 mo of cell age, newborn neurons transiently demonstrate electrophysiological properties that differ from mature GCs. Lower firing thresholds make this population more excitable and more likely to undergo LTP (Ge, Yang, Hsu, Ming, & Song, 2007; Schmidt-Hieber, Jonas, & Bischofberger, 2004), thus suggesting a critical period for synaptic modification and learning. These newborn neurons eventually become identical to mature GCs. Adult neurogenesis is ongoing throughout life (Kuhn, DickinsonAnson, & Gage, 1996), and therefore new cohorts of newborn neurons are continually generated and capable of undergoing behaviorally-induced synaptic modification during their critical period. Finally, a few studies indicate the preferential or at least equivalent recruitment of newborn neurons into functional hippocampal circuitry (Kee, Teixeira, Wang, & Frankland, 2007; Ramirez-Amaya, Marrone, Gage, Worley, & Barnes, 2006; Stone et al., 2011). In the Morris water task, preferential activation of newborn neurons is maximal between 6-8 weeks. Newborn neurons at this age are more than twice as likely to fire compared with mature neighbors (5% vs 2%), but this preferential recruitment declines to 3.5% by 8 weeks cell age (Kee et al., 2007). Taken together, current knowledge on the proportion of adult-generated neurons added to the DG, the distinguishing electrophysiological properties of newborn neurons during a critical window, and the participation of newborn neurons in hippocampal memory circuitry are compatible with the possibility that the most recently generated GCs make up or at least disproportionately contribute to the excitable population in the DG.

Adult neurogenesis in the DG occurs throughout the lifespan, but the rate of cell addition decreases dramatically with age. In the rat, the total granule cell number increases by 35-43% between one month and one year of age (Bayer, 1982). The rate of proliferation peaks in the second week of life, during which an estimated 50,000 new granule cells are added per day (Schlessinger, Cowan, & Gottlieb, 1975). In contrast, neurogenesis in young adult rats (9 mo) occurs at a rate of 9,000 cells per day (Cameron & McKay, 2001) and persists at a very low rate for the remainder of life (Kempermann, 2006; Kuhn et al., 1996).

Given that production of adult born neurons is a strongly age dependent process, it follows that the DG of very young rats may contain a large proportion of recently generated, and presumably more excitable, granule cells, while in adults this population is relatively much smaller. If the total number of simultaneously active cells is kept relatively constant, for instance through inhibitory regulation, then the larger pool of potentially excitable cells in juveniles might lead to a greater selectivity in the subsets of activated cells when the rats are exposed to multiple environments and, correspondingly, lead to less overlap across environments. In CA3 and CA1, populations may exhibit activation probabilities as expected through random sample with replacement, due to the lack of evidence for adult neurogenesis in these regions. Another major goal of the present study was to test the hypothesis that the juvenile DG granule cell population possesses a significantly lower activation probability (P_1) due to higher selectivity in the identity of the active subpopulations during spatial encoding, whereas for CA3 and CA1 principal neurons, P_1 may be similar between the two age groups.

D. Quantifying neural activation patterns using the *Homer1a* immediate-early gene: methodological overview

The principal neurons in the DG, CA3, and CA1 subfields fire action potentials when the animal moves through specific locations in space to which they are attuned, called place fields (O'Keefe & Dostrovsky, 1971). Any given 2-dimensional space is spanned by numerous place fields, so that when an animal moves through the environment, a neural population or 'neural code' corresponding to the representation of that space emerges. Place fields are normally established within the first visit to an environment (Hill, 1978; Wilson & McNaughton, 1993), and this representation remains stable during subsequent visits and in response to minor changes in environmental cues (Muller & Kubie, 1987).

In the present study, to maximize chances of evoking activity across different subsets of neurons, the animals ran on two different sized circular tracks connected by a bridge and located in the same room. The large track (*X4*) was four times the area of the small track (*X1*). During training, the animals moved between the two tracks via a connecting bridge to ensure that each track was represented by a unique subpopulation of neurons (Colgin et al., 2010). The connecting bridge was intentionally longer than the average place field diameter in the dorsal hippocampus (Maurer, Cowen, Burke, Barnes, & McNaughton, 2006). This paradigm was previously employed in ensemble recordings in the CA3 and CA1 regions to produce uncorrelated place maps (the degree of population overlap was not reported) (Colgin et al., 2010); although it is, in principle, possible for the same subpopulation of neurons to have uncorrelated place field maps

merely by field rearrangement rather than massive substitution in the membership of the active population.

Fluorescence *in situ* hybridization (FISH) for immediate-early genes is widely used as a reliable marker for visualizing large-scale neural activity. The immediate-early gene *Homer1a* (*H1a*) is tightly coupled to plasticity-inducing neural activity (Brakeman et al., 1997; Cole, Abu-Shakra, Saffen, Baraban, & Worley, 1990; Kato, Ozawa, Saitoh, Hirai, & Inokuchi, 1997) and its transcription kinetics provide an appropriate window for conducting a behavioral task such as track running (Vazdarjanova & Guzowski, 2004; Vazdarjanova, McNaughton, Barnes, Worley, & Guzowski, 2002). *H1a* is the short isoform in the Homer family, which also consists of constitutively expressed genes (*H1b/c*) (Bottai et al., 2002). Homer proteins are located in postsynaptic densities (PSD), where long H1b/c forms bind with protein targets (such as ionotropic and metabotropic glutamate receptors) involved in intracellular Ca^{2+} signaling and other synaptic modification processes. H1a disrupts the protein clusters through competitive binding of H1b/c protein targets, which reduces glutamate-induced Ca^{2+} release at the postsynaptic site (Shiraishi-Yamaguchi & Furuichi, 2007; Xiao, Tu, & Worley, 2000). In addition, the growth of dendritic spines and synapses is disrupted by H1a expression, suggesting that the protein acts to regulate structural modifications through an activity-induced feedback loop (Sala et al., 2003; Xiao et al., 2000).

This study sought to determine whether the DG, CA3, and CA1 hippocampal populations indeed contain uniformly excitable cells by comparing the empirically derived P_1 values with those predicted by random sample with replacement. By

comparing the P_1 of principal neurons in prepubescence and adulthood, the present study also aimed to determine the effect of development on hippocampal pattern separation. Neurons active during track running were identified by the presence of discrete transcription foci within the nucleus (Guzowski et al., 1999). The number of neurons active on the large track divided by the number active on the small track was applied to the unbiased estimator method (Alme et al., 2010) to calculate actual P_1 values (see Methods for details). The P_1 value reflects a network's ability to allot orthogonal subpopulations to encode for different input patterns. Low P_1 values correspond to less overlap across contexts, and therefore potentially enhanced ability for pattern separation.

CHAPTER 2 MATERIALS AND METHODS

A. Subjects and handling procedures

The handling and testing procedures in this study were consistent across six cohorts of 10 rats of the same age; each cohort consisted of 3 caged controls (HC), 3 small track runners (X1), 3 large track runners, and 1 positive gene expression control (MECS). Thirty adult (4.5-5.5 mo) and thirty juvenile (P28) naive, male Long-Evans rats were housed in pairs or triplets on a 12-h light-dark cycle with *ad libitum* access to water and food. The rats were handled twice daily for one week before the experiment to ensure habituation to handling procedures.

Starting one week before testing, the animals were placed on mild food restriction to motivate track running; imitation chocolate sprinkles (Cake Mate® brand) were given as food reward. Adult rats (mean weight of 579 g) were around 90% of their free-feeding weight; juveniles (mean weight of 86 g) were within the expected weight range of free-feeding pups to ensure normal cognitive and motor development (see Appendix for food restriction details).

B. Circular tracks and training procedures

Two circular tracks were constructed from wood and painted grey, with no obvious markings (Figure 2.1). Each apparatus consisted of a 12.7 cm wide track, raised 16.8 cm from the ground, with a 5.1 cm 'lip' along its edge to prevent the rat from slipping off. The circumference and area of the large track was four times that of the

small track (*C*: 342.8 cm and 86.0 cm; *A*: 0.44 m^2 and 0.11 m^2). The tracks were located in the same experiment room (see Appendix for room description).

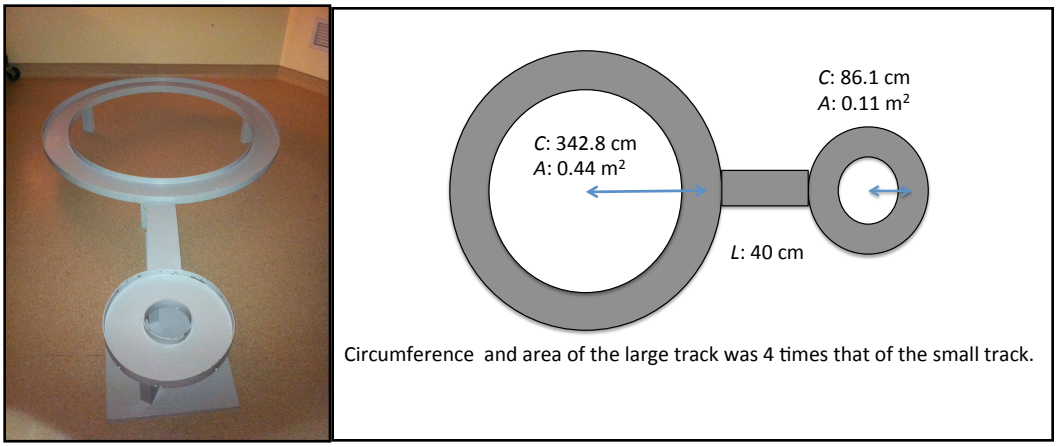

Figure 2.1 Image and schematic (not to scale) showing the circular tracks and connecting bridge.

Each rat was trained twice daily for 5 days on the tracks in the same room used in testing. For a training session, the rat was transported from the animal housing room to the experiment room in a covered plastic box. The holding box had opaque walls and limited space for exploration but did not restrict the rat's movement (29.2 cm x 18.7 cm x 15.2 cm for adults; 18.7 cm x 14.3 cm x 8.3 cm for juveniles; see Appendix for details regarding box construction). Each rat was habituated to being in the dark boxes for up to 2 h to minimize behaviorally uncorrelated immediate-early gene (IEG) expression, such as from sustained IEG transcription in hippocampal granule cells (Chawla et al., 2005). The rats engaged in quiet wakefulness or rest when in the dark boxes.

Days 1-3 of training involved a 10 min session twice daily, during which each rat moved between the two tracks via a 40 cm long wooden bridge (same width and height as the tracks) in the clockwise direction on each track. Wooden blocks that could obstruct

the track passage were used to help guide the rat in the correct direction. Food reward was given at random locations on the track.

For days 4-5 of training, the tracks remained in the original configuration and location in the experiment room, but the connecting bridge was removed. Twice daily, each animal ran unidirectionally on one track for 5 min, was carried (uncovered) to the other track, and ran unidirectionally for another 5 min. Half of the animals were pseudo-randomly chosen to always begin training on the larger track, while the remaining rats always began on the smaller track.

On experiment day, each rat, regardless of treatment, spent a minimum of 1 hr in the dark box in the testing room prior to behavior, in order to establish baseline *Homer1a* (*H1a*) gene expression. Behavioral groups ran for 5 min unidirectionally on either the large circular track (*X4*, $n = 9$) or small circular track (*X1*, $n = 9$), then returned to their dark holding box for 24 min before covered transport to the perfusion room. The tracks were cleaned with 70% ethanol between rats. Within the 5 min test session, the adult group ran an an average of 9.6 ±1.6 laps on the large track and 13.0 ± 2.9 laps on the small track; the juvenile group ran an average of 13.0 ± 1.0 laps on the large track and 22.7 ± 5.7 laps on the small track. Control groups consisted of a negative gene expression home cage group (*HC*, $n = 9$), which was directly sacrificed after spending a minimum of 1 h in the dark box, and a positive gene expression group (*MECS*, $n = 3$), which received a maximal electroconvulsive shock (MECS) in place of track exposure and was returned to their dark box (see Appendix for constant-current generator settings). MECS treated animals exhibit robust *H1a* gene expression in principal neurons across different brain

regions, including the hippocampus, (Cole et al., 1990) and therefore serve as the technical positive control during fluorescence *in situ* hybridization (Guzowski et al., 1999).

C. Tissue extraction and sectioning

At 24 ½ min following the end of behavior, each rat was anesthetized using isoflurane and subcutaneously injected with sodium pentobarbital (1 ml for adults; 0.5 ml for juveniles). Each rat underwent transcardiac perfusion-fixation using ice cold 1X phosphate buffered saline (PBS) and 4% paraformaldehyde (PFA). Solutions were made with RNase-free water. Each brain was extracted within 5 min after perfusion and cut along the midline. The hemispheres were submerged in cold 4% PFA for 2 h post-fixation at 4 ^{o}C; switched into 30% sucrose in 1X PBS until they sank (around 48 h); then frozen and stored at -80 ^{o}C.

For each cohort, a right hemisphere from each rat was included in a tissue block made with Tissue-Tek® O.C.T.™ compound, and 40 μm thick sections were captured through the dorsal hippocampus in the coronal plane using a Leica cryostat (Model CM3050 S). Sections were thaw-captured on superfrost-plus slides (Fisher Scientific), dried at room temperature, and stored at -80 ^{o}C (see Appendix for additional details). All four behavioral conditions were represented on a single slide.

D. Fluorescence in situ hybridization

The sections containing the dorsal hippocampus were processed in two batches of fluorescence *in situ* hybridization (FISH). The sections for both age groups were processed together in the same batch, and all four behavioral conditions for an age group were represented on one slide. These measures were taken so that all brains were similarly processed and to avoid incurring systematic errors in any single group.

Single-label FISH for the IEG *H1a* was performed as described previously (Bottai et al., 2002; Vazdarjanova & Guzowski, 2004; Vazdarjanova et al., 2002), with the addition of proteinase K buffer applied after the initial tissue fixation step. Target mRNA transcripts were stabilized with 4% PFA, and the slides were incubated with 0.3% proteinase K buffer to increase permeability of the tissue and improve accessibility to the target transcript. A series of washes and subsequent incubation with pre-hybridization buffer limited non-specific binding of the probe and lowered the background noise. The hapten-labeled antisense riboprobes specifically hybridized with the target 3' UTR of the *H1a* mRNA transcript over 14-16 h. The sections were quenched with 2% H_2O_2 to limit background labeling, and the HRP (horseradish peroxidase)-antibody conjugate bound to the riboprobe hapten sites overnight. For improved visualization under fluorescence imaging, fluorescein-tyramide dye was used to amplify the fluorophore signal. Nuclei were counterstained with DAPI (4'-6-diamidino-2-phenylindole) to colocalize the apparent transcription foci with a neuron. Finally, the slides were coverslipped using Vectashield (Vector Labs) and sealed. (See Appendix for complete FISH procedure.)

E. Image acquisition and pre-processing

Image stacks of the dorsal hippocampus (Bregma -3.00 to -4.00 mm; see Figure 6.1 for brain atlas depiction) were captured using an Olympus FluoView FV1000 confocal microscope at 1 μm step-size using a 40X oil objective. The FITC (fluorescein isothiocyanate) high voltage (HV) laser setting was kept constant for all image stacks from a single slide. This setting was optimized for detecting bright intranuclear signal based on the cage control section on each slide; it was determined by avoiding signal saturation in the middle z-layer ± 2 layers. DAPI intensity varied with hippocampal region (CA3 neurons were typically fainter than CA1 and DG neurons) and with depth into the tissue; thus, to optimally visualize the nuclei, the DAPI HV setting in each section and region of interest was determined in the same manner as the FITC setting.

The Olympus FluoView Multi-Area Time Lapse program was used to capture non-overlapping stacks in the dentate gyrus (DG), CA3, and CA1 regions. Between 3-5 slides/animal were imaged. Since the lower blade of the DG has been shown to exhibit little to no behaviorally-induced IEG expression (Chawla et al., 2005), image acquisition and analysis was only of the upper blade.

The confocal image stacks were saved in 8-bit RGB TIFF format. The distribution of the green and blue pixel greyscale values showed no bleed-through into the green channel. In both channels, however, pixels did not appear for greyscale values less than 7 on a 0-255 scale (black is 0; white is 255), indicating the possible presence of electronic noise or stray photons. The lower limit of the image display range was reset to 7 from the look-up table (LUT) to offset the noise contribution in the signal.

F. Automated transcription foci quantification

Automated quantification of *H1a* intranuclear foci (INF) in the image stacks was performed using the *IEG Analysis* software (written in Java script; developed through plugin-ins for ImageJ). The main steps of the software algorithm for identifying each INF are summarized. The algorithm assumes that each INF contains a maximum in pixel intensity (I_{max}), in the form of a single or group of connected pixels. The local maximum must fulfill two user-specified thresholds, the minimum green intensity (G_{min}) and the minimum blue or background intensity (B_{min}), in that $I_{max} \geq G_{min}$ and $I_{max} \geq B_{min}$. The G_{min} value ensures that a pixel has to have a certain green intensity value to be considered FISH signal, and anything lower is considered noise; furthermore, the B_{min} value ensures that potential intranuclear FISH signal is colocalized with DAPI staining or excluded as noise. When a local maximum is determined, each of its connected pixels in 3D space are evaluated against the G_{min} and B_{min} criteria as a potential component of the INF object. If an overlap in INF objects is detected, the region of overlap is determined based on the Gaussian distribution fit for the pixel intensity values, and the objects are segmented.

The final putative FISH signal satisfied all the user-specified thresholds in the following parameters: minimum green intensity, minimum peak green intensity, minimum blue intensity, minimum percent blue, minimum foci volume, and minimum foci z-layers. These thresholds were determined empirically by sampling stacks from across behavioral groups and brain regions. For instance, the G_{min} and B_{min} values were determined in ImageJ by measuring the typical intensity ranges for DAPI and FITC signal. The results of *IEG Analysis* quantification using these values were visually

inspected in sampled stacks, and the values were adjusted if necessary until the final thresholds were determined. The other parameters were determined in similar manners. (see Appendix for specific threshold values.)

For automated foci quantification, all threshold values were kept constant across age, treatment, and region in the analysis. Foci characteristics were generated for each identified INF object, including foci volume, average foci intensity, maximum foci intensity, and integrated foci intensity (see Appendix for full list). Analyses were limited to only the foci in the median 20% of an image stack to avoid sampling from partial or damaged cells (Vazdarjanova et al., 2002). Without available methods for determining the number of nuclei, foci counts were normalized by volume of the sampled molecular layer (see Appendix for details).

G. Unbiased estimation of neuronal activation probability

The unbiased estimator method was used to calculate the independent probability of a neuron being allocated to an environment (P_1) (Alme et al., 2010). Normally, the activation probability is estimated as the number of activated cells divided by the total number of anatomically quantifiable cells (*tot*). This method introduces potential bias as it assumes that all cells are equally capable of activation. In the unbiased method, the number of neurons activated during exposure to n distinct environments (X_n/tot) over the number activated during exposure to one environment (X_1/tot) forms X_n/X_1, in which the total number of cells cancels out. The unbiased estimator method involves solving for the

variable P_1 in the polynomial equation $\frac{X_n}{X_1} = \frac{1-(1-P_1)^n}{P_1}$, given the empirically derived values for X_n and X_1 and $n = 4$. P_1 can alternatively be determined graphically by plotting the polynomial curve for $\frac{X_n}{X_1} = \frac{1-(1-P_1)^n}{P_1}$ vs. P_1 and finding the corresponding P_1 value for the empirical X_n/X_1 ratio. In this study, X_n and X_1 corresponded to the number of neurons active on the large and small track, respectively.

H. Statistical analyses

Effects of treatment and age on gene expression and foci characteristics were evaluated by analysis of variance tests (ANOVA). When a main effect was present at the $\alpha = .05$ level, additional comparisons were performed with the Tukey-Kramer post hoc test (Statview).

CHAPTER 3 RESULTS

To examine how experience and development influence behaviorally-induced activity in the hippocampal population, the neuronal activity marker *Homer1a (H1a*) was quantified in juvenile (P28) and adult rats following track running behavior. The effect of environment size on population activity was concurrently examined by using two different sized tracks: the large track (*X4*) was four times the area of the small track (*X1*). It is well documented that principal neurons in the dentate gyrus (DG), CA3, and CA1 regions exhibit behaviorally-correlated place selective firing (O'Keefe & Dostrovsky, 1971; Wilson & McNaughton, 1993) that induces rapid induction of immediate-early gene transcription specific to the activated cells (Cole et al., 1990; Guzowski et al., 1999). The presence of *H1a* intranuclear transcription foci thus provides a neural marker for quantifying the activated population in each brain region of interest. Because no method of automated nuclear segmentation was available for this study, the transcription foci counts were normalized by the sampled volume in the molecular layer (in units of foci per cubic mm) to enable comparisons across animals. Unfortunately, this does not provide an estimate of activation probability relative to the actual number of neurons. Nevertheless, since only the cell layers were analyzed, the numbers of observed foci are at least ordinally consistent with known differences in activity sparsity in the hippocampal subregions, in that DG < CA3 < CA1.

A. Effects of experience and age on gene expression in the hippocampus

A 3x2 randomized-groups ANOVA was performed on activity-induced early gene expression in principal neurons for the DG, CA3, and CA1 regions (Figure 3.1, 3.2). The

behavioral conditions consisted of home cage (*HC*), small track running (*X1*), and large track running (*X4*). Of the 35 rats sampled, 13 were juveniles (P28) and the rest were adults (4.5-5.5 mo)[1]. Heterogeneity of variance was noted in the CA3 data. The obtained probability levels for effect of behavior and age were far beyond the preset $\alpha = .05$, but the influence of the behavior-by-age interaction was misleadingly amplified; therefore, a log transformation was performed on CA3 gene expression values to achieve homogeneity of variance for analyses.

DG granule cells exhibited similar levels of gene expression across all levels of behavioral condition and age. There was no significant interaction between behavior and age; although, there was a trend for limited increases in net expression with increase in environment size (Figure 3.1A, 3.2A).

In the CA3 subregion, statistically significant differences in gene expression were evident between the juvenile and adult age groups, averaged over the three behavioral conditions [$F(1,29) = 15.586$, $p = .0005$]. There was a smaller, but still statistically significant difference among the behavioral conditions, averaged over the two age groups [$F(2, 29) = 4.549$, $p = .0191$]. A behavior-by-age interaction was not present. All pairwise comparisons among means were performed using a post hoc Tukey-Kramer method at $\alpha = .05$. These comparisons showed that mean CA3 gene expression in the juveniles was significantly higher than in the adults; additionally, running on the large track induced significant up-regulation of gene transcription relative to caged controls (3.1B, 3.2B).

---

[1] Juvenile group: home cage (*HC*, $n = 4$), small track (*X1*, $n = 6$), and large track (*X4*, $n = 3$). Adult group: *HC*: $n = 8$, *X1*: $n = 7$, and *X4*: $n = 7$.

In CA1, there was strong statistically significant effect of behavioral condition on gene expression [$F(2, 29) = 18.899$, $p < .0001$]; running on the large track induced significantly more gene expression than the home cage condition (3.1C, 3.2C). Averaging across all behavioral conditions, CA1 gene expression was also highly dependent on age [$F(1,29) = 9.904$, $p = .0038$]; juveniles exhibited significantly more expression than adults (Figure 3.1C, 3.2C). The behavior and age variables affected gene expression independently of one another, however.

In summary, the data strongly suggest that experience and age act independently to influence the amount of activity-induced *Homer1a* early gene transcription in CA3 and CA1. In both regions, running on the large track evoked greater gene expression relative to home cage controls; additionally, juveniles exhibited greater gene expression averaging across the behavioral conditions compared to adults. In contrast, gene expression in DG granule cells exhibit no significant influence of age and very limited *Homer1a* gene up-regulation in response to manipulations in experience.

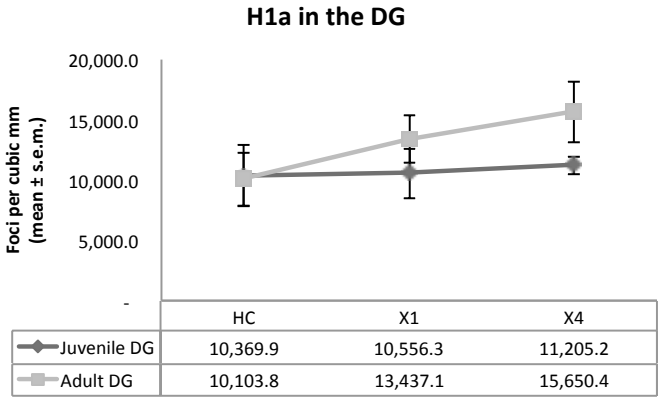

Figure 3.1A Number of *H1a* foci with respect to experience and age in the DG.

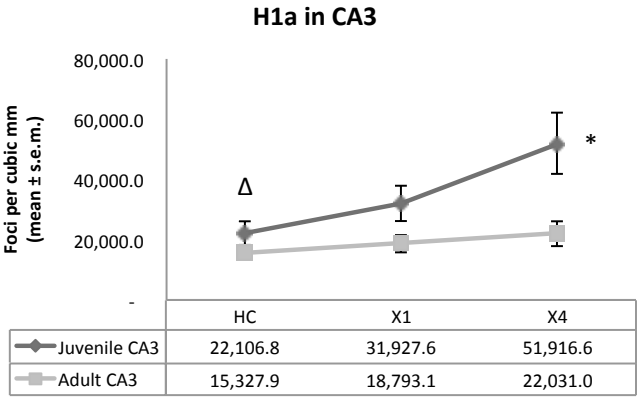

Figure 3.1B Number of *H1a* foci with respect to experience and age in CA3.
Significantly more *H1a* foci in *X4* condition, relative to *HC* (Δ $p < .05$); significantly more foci in juveniles (* $p < .05$)

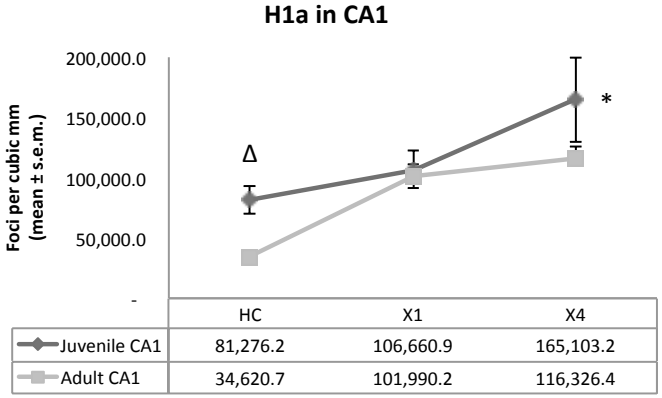

Figure 3.1C Number of *H1a* foci with respect to experience and age in CA1.
Significantly more *H1a* foci in *X4* condition, compared to *HC* (Δ $p < .05$); significantly more *H1a* foci in juveniles compared to adults (* $p < .05$)

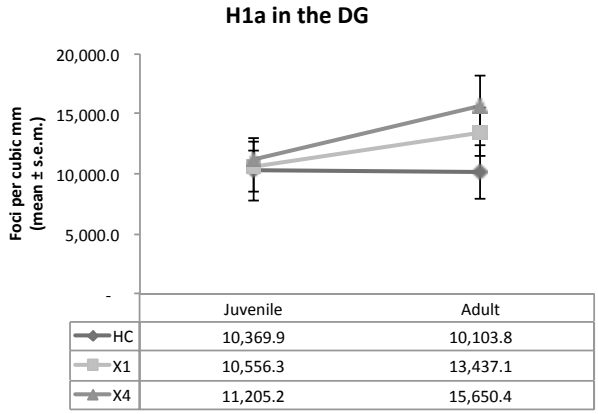

Figure 3.2A Number of *H1a* foci with respect to experience and age in the DG. Same data as Figure 3.1A, plotted on switched axes.

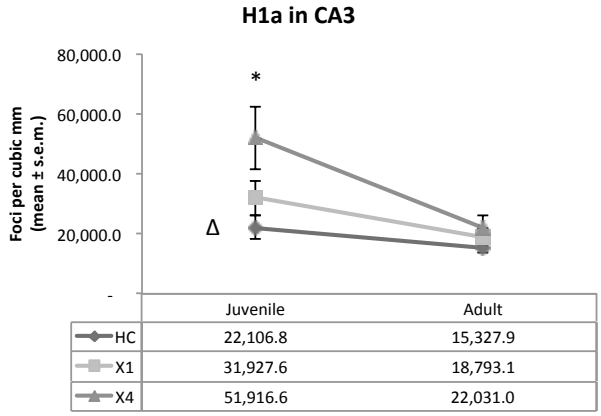

Figure 3.2B Number of *H1a* foci with respect to experience and age in CA3. Same data as Figure 3.1B, presented on switched axes.

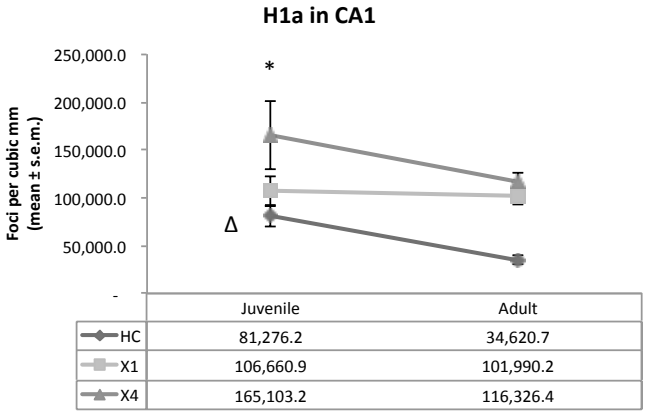

Figure 3.2C Number of *H1a* foci with respect to experience and age in CA1. Same data as Figure 3.1C, presented on switched axes.

B. Unbiased activation probability of hippocampal neurons

The empirical X_n/X_1 value for each region of interest was determined by either directly dividing the gene expression on the large track by the gene expression on the small track or first adjusting for home cage expression.

In adults, the home cage adjusted ratios yielded P_1 values of 0.58 (DG), 0.48 (CA3), and .83 (CA1) (Figure 3.4A) (see Methods for calculation details). The direct *X4/X1* calculations produced ratios close to 1, which had corresponding activation probabilities (P_1) of ~0.85 for all three hippocampal subregions (Figure 3.3A). For DG granule cells, the calculated P_1 values (0.58 and 0.85) were an order of magnitude larger than the ~0.01 anatomical estimate predicted by random sampling (Chawla et al., 2005). The home cage adjusted P_1 values for CA3 and CA1 were both higher than expected from electrophysiological recordings (0.20 and 0.40; Guzowski et al., 1999; S. Leutgeb, Leutgeb, Treves, Moser, & Moser, 2004). The excitation relationship between the two regions, however, was conserved in that CA1 neurons are roughly twice as likely to be active in a given environment as CA3 neurons (Figure 3.4A).

In juveniles, using the standard correction method for home cage expression, X_n/X_1 calculations produced corresponding activation probabilities of -0.08 (DG), 0.18 (CA3), and 0.13 (CA1), while uncorrected *X4/X1* calculations yielded probabilities of 0.94, 0.60, and 0.63 (Figure 3.3B and 3.4B). In the DG, the direct *X4/X1* calculation yielded an excitation probability near 1, which would result in nearly identical encoding populations given two environments (Figure 3.4B). The home cage adjusted calculation, conversely, corresponded to a very small probability of activation near 0 (Figure 3.5B).

The juvenile CA3 P_1 value was consistent with the electrophysiological estimate of 0.20; both CA3 and CA1 P_1 values were much lower in juveniles relative to adults (Figure 3.4A-B).

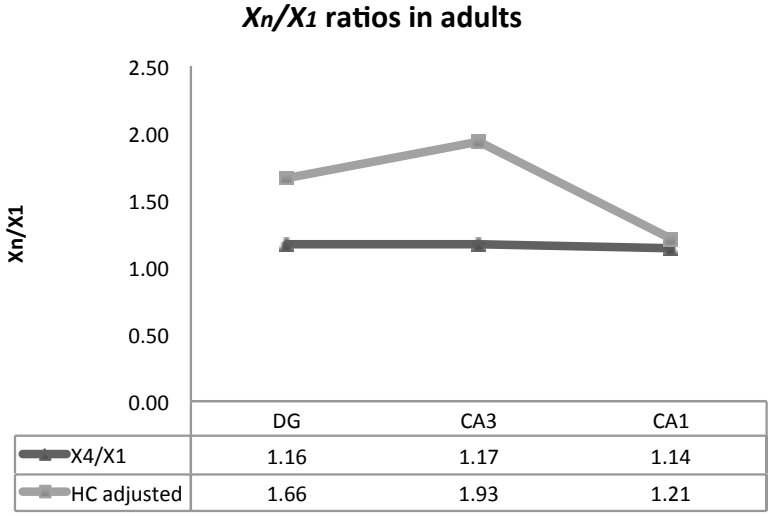

Figure 3.3A X_n/X_1 ratios for adults. The light grey line indicates the calculated X_n/X_1 ratios after subtracting home cage expression from the behavioral expression.

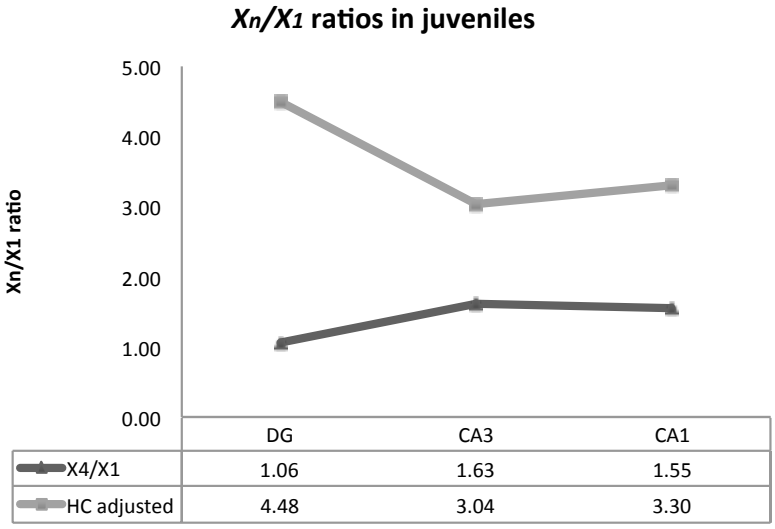

Figure 3.3B X_n/X_1 ratios for juveniles. The light grey line indicates X_n/X_1 ratios after subtracting home cage expression from the behavioral expression.

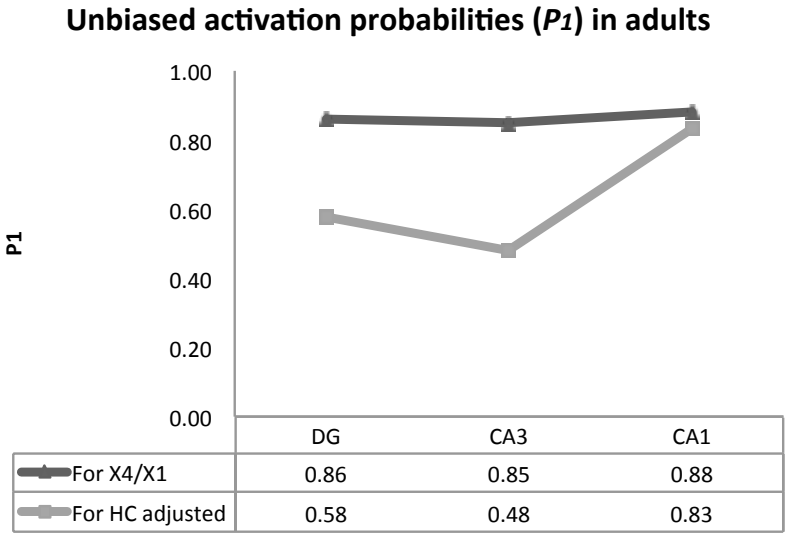

Figure 3.4A Unbiased activation probabilities for adults. The light line indicates P_1 values corresponding to X_n/X_1 ratios calculated after subtracting home cage expression from the behavioral expression.

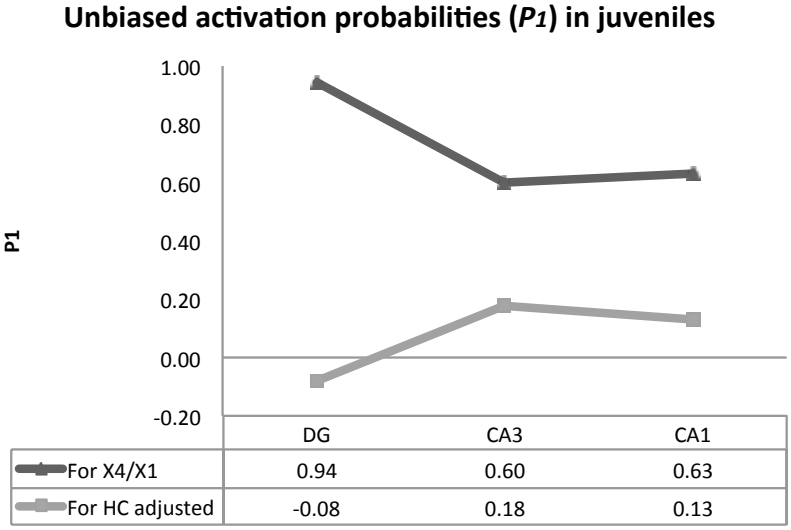

Figure 3.4B Unbiased activation probabilities for juveniles. The light grey line indicates P_1 values corresponding to X_n/X_1 ratios calculated after subtracting home cage expression from the behavioral expression.

C. Effects of age and experience on hippocampal foci characteristics

Traditional studies using immediate-early genes (IEGs) as markers for neural activity interpret the data in a binary fashion. A neuron is categorized as having been active or inactive in a behavioral context based only on whether intranuclear transcription foci are present, with no information on how much or how little activity occurred. There is evidence, however, that electro-transcriptional coupling (ETC) relates the number of spikes fired by a neuron with the amount of IEG mRNA transcripts present at the transcription site (Guzowski et al., 2006). This raises the possibility that the extent of activity of a neuron may be discernible through more detailed analysis of foci characteristics.

Volume per transcription focus refers to the number of continuous green pixels attributed to an intranuclear focus in a 3-dimensional image stack. The integrated intensity is the sum of all FITC intensity values in a transcription focus. The average integrated intensity is the sum of the intensities for all foci in a regional of interest divided by the total number of identified foci. Both characteristics are related to the amount of mRNA transcripts present at the transcription site as a result of neuronal activation. In preliminary analyses, foci volume appeared to be highly correlated with integrated intensity; therefore, further analyses focused on integrated intensity since it may more accurately reflect the amount of mRNA within a nucleus by considering the combined effects of volume and intensity.

A 3x2 randomized-groups ANOVA was performed on the integrated intensity of putative intranuclear transcription foci in principal neurons for the DG, CA3, and CA1

regions. The behavioral conditions consisted of home cage (*HC*), small track running (*X1*), and large track running (*X4*). Foci were pooled from the same 35 rats used to examine effects of experience and age on boolean gene expression (adults, $n = 22$; juveniles, $n = 13$). Heterogeneity of variance was noted in the DG and CA1 data. Although the probability levels for effect of experience and age were far beyond the preset $\alpha = .05$, a log transformation was performed on the data to achieve homogeneity of variance to more accurately quantify potential behavior-by-age interactions.

In the DG, there was a significant difference in mean integrated foci intensity among the behavioral conditions, averaged over the two age groups [$F(2, 29) = 14.672$, $p < .0001$]. Pairwise comparisons using the post hoc Tukey-Kramer method at $\alpha = .05$ showed that running on either circular tracks induced significantly larger and brighter foci relative to caged controls (Figure 3.5A, 3.6A).

There was also a strong significant effect of behavioral condition on integrated intensity in CA3 [$F(2,29) = 16.187$, $p < .0001$], averaging across age groups. The Tukey-Kramer post hoc test showed significant differences between the mean integrated intensities for foci from the home cage and both running groups, as well as between the small track and large track groups (Figure 3.5B, 3.6B).

Similarly in CA1, there was a significant influence of behavioral conditions on integrated intensity values [$F(2,29) = 55.304$, $p < .0001$]. There was also a significant difference between the juvenile and adult age groups averaged over the three behavioral conditions [$F(1,29) = 13.669$, $p = .0009$]. These main effects were accompanied by a significant behavior-by-age interaction [$F(2,29) = 4.185$, $p = .0253$], which indicated that

the effect of experience differed between the age groups. Post hoc Tukey-Kramer at $\alpha = .05$ showed that running on either track produced significantly bigger and brighter foci relative to caged controls; additionally, the mean CA1 integrated intensity in the adults was significantly higher than in the juveniles (Figure 3.5C, 3.6C).

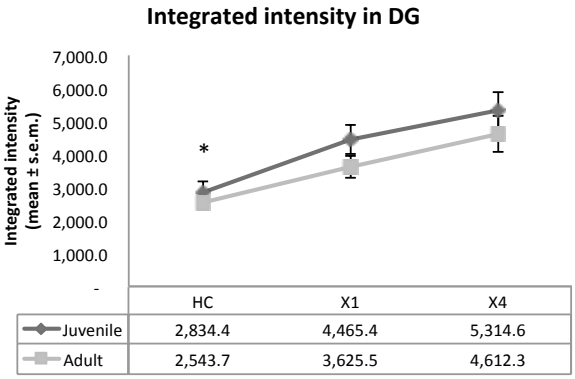

Figure 3.5A DG integrated intensity as a function of age and experience. Running on either circular tracks induced significantly larger and brighter foci relative to caged controls (* $p < .05$)

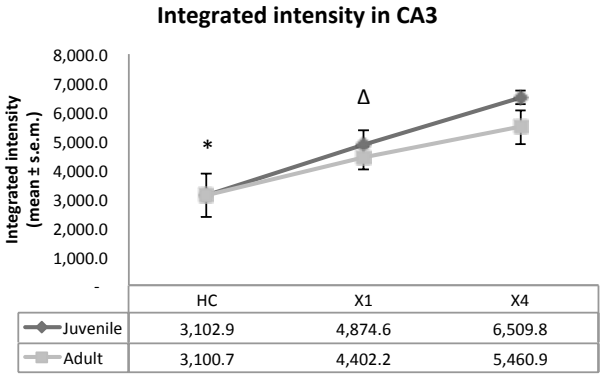

Figure 3.5B CA3 integrated intensity as a function of age and experience. Significantly higher integrated intensity for *X1* and *X4* conditions relative to *HC* (* $p < .05$); significant difference between the *X1* and *X4* conditions ($\Delta\, p < .05$)

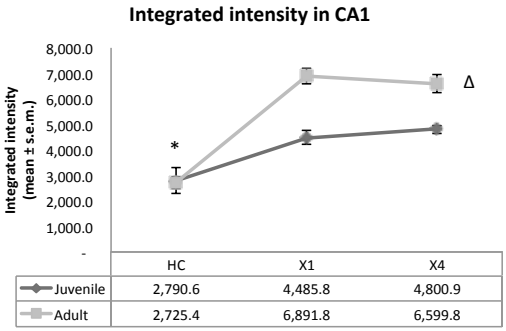

Figure 3.5C CA1 integrated intensity as a function of age and experience. Significantly higher integrated intensity for *X1* and *X4* conditions relative to *HC* (* $p < .05$); significantly higher integrated intensity in adults, compared to juveniles ($\Delta\, p < .05$); significant experience-by-age interaction effect.

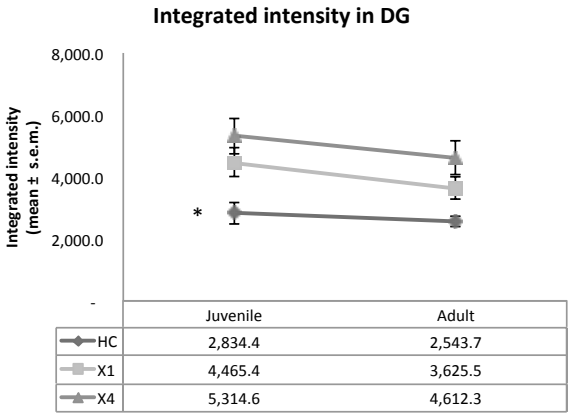

	Juvenile	Adult
HC	2,834.4	2,543.7
X1	4,465.4	3,625.5
X4	5,314.6	4,612.3

Figure 3.6A DG integrated intensity as a function of age and experience. Same data as Figure 3.5A, presented on switched axes.

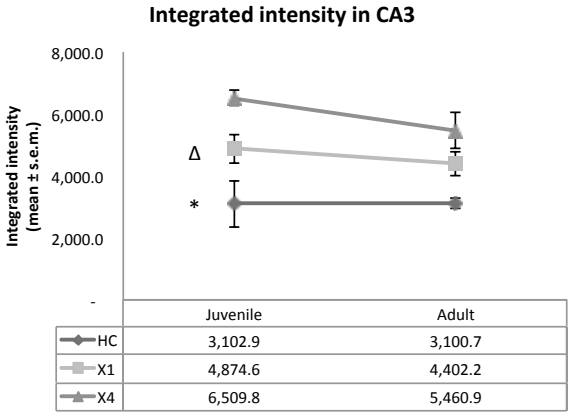

	Juvenile	Adult
HC	3,102.9	3,100.7
X1	4,874.6	4,402.2
X4	6,509.8	5,460.9

Figure 3.6B CA3 integrated intensity as a function of age and experience. Same data as Figure 3.5B, presented on switched axes.

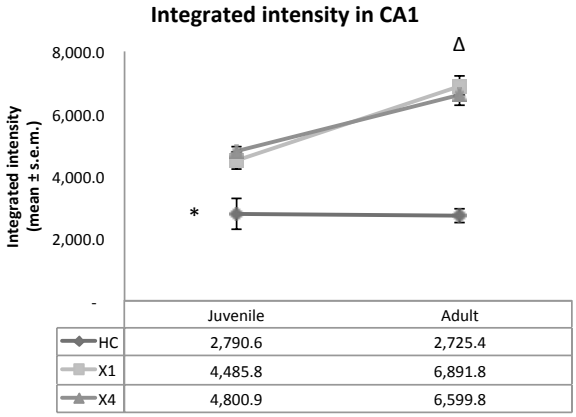

	Juvenile	Adult
HC	2,790.6	2,725.4
X1	4,485.8	6,891.8
X4	4,800.9	6,599.8

Figure 3.6C CA1 integrated intensity as a function of age and experience. Same data as Figure 3.5C, presented on switched axes.

CHAPTER 4 DISCUSSION

To investigate the effects of experience and development on activity patterns in the hippocampus, the *Homer1a* immediate-early gene was used as a marker for neuronal activation in juvenile (P28) and adult rats (~5 mo) in a track running paradigm. The main finding was that, using the standard correction for home cage expression, the probability of activation in juveniles was substantially lower relative to adults across not only the DG, but also the CA3 and CA1 subregions, suggesting enhanced orthogonality in the encoding populations in the juvenile hippocampus.

For the juvenile DG, the unbiased estimation for probability of activation after home cage adjustment yielded a P_1 value near 0, versus 0.58 in adults (Figure 3.4A-B). Due to an inherent margin of error, the DG X_n/X_1 ratio was greater than the large-to-small-track area ratio of 4, thus incurring a small negative value. Treating the holding box as a small, additional environment exposure (Alme et al., 2010) would increase the total area of the exploration to slightly larger than 4, and consequently modify the activation probability into a small positive number. The small P_1 in juveniles corresponds to higher selectivity in the membership of the active population, while the large P_1 in the adults indicates that many of the same cells are active across different environments. The present finding that the granule cell population in adults has an activation probability of 0.58 confirms previous observations that, across multiple environment exposures, there is substantial overlap in the active subpopulation (Alme et al., 2010). For each region, the proportion of neurons active under each condition was calculated by dividing the foci count from experience by the MECS foci count to obtain an estimate of the proportion of

anatomically active neurons (Figure 6.3, 6.4; see Appendix). In the adult DG, as expected (Chawla et al., 2005; Jung & McNaughton, 1993), 2-4% of granule cells were active in the behavioral context. Despite this apparent sparse coding, the high probability of overlap found across environments suggests that activation within this excitable population is non-sparse. These findings are consistent with the early retirement theory's hypothesis that, within the adult DG population, relatively few numbers of neurons participate in the encoding of many events while the vast majority of neurons exhibit little to no activity in an environment.

The low activation probability in DG found in juveniles appears consistent with the hypothesis that postnatally generated, hyper-excitable granule cells may contribute significantly to excitability within the GC population. The large influx of newborn neurons early in life appears to promote enhanced selectivity within the pool of potentially excitable neurons, thus resulting in an activation probability near 0 that a single neuron will be selected to fire in an environment. In juveniles, this activation probability is highly sparse and resembles the value predicted by random sampling from within a uniformly excitable population. As the rate of neurogenesis declines in adulthood, the subpopulation of potentially excitable cells becomes greatly reduced and appears to result in a highly nonuniform distribution of excitability in the adult DG. The substantially lower P_1 value in juveniles indicates that sparse, but non-overlapping subpopulations, participate in encoding events. Since sparse, orthogonal coding enhances a population's ability to decorrelate input patterns (Marr, 1971; McNaughton & Morris,

1987), the findings suggest that juveniles likely possess greatly enhanced capability for pattern separation (Figure 4.1).

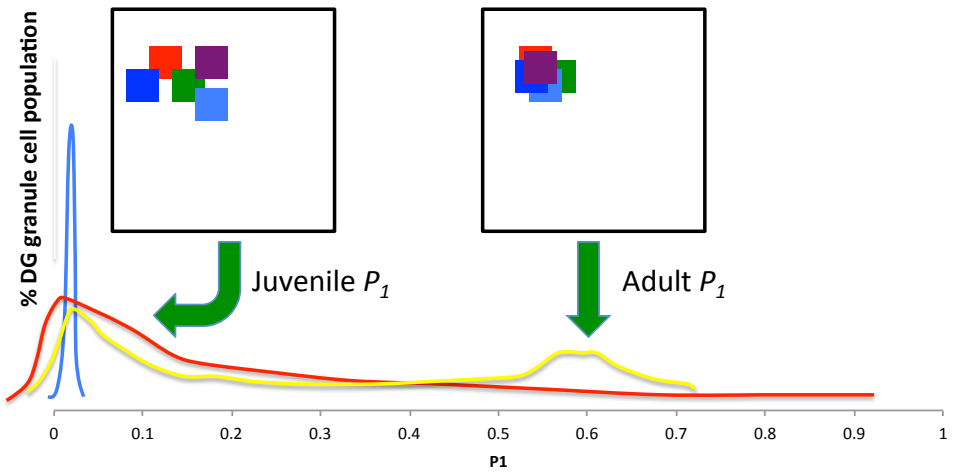

Figure 4.1 Possible distributions of probability of activation within the DG population. The narrow curve with peak near 0 depicts the cartoon distribution of a uniformly excitable population with little variation in probability values, which possibly reflects the excitability distribution in the juvenile DG based on the empirical low activation probability in the region. The broader, more distributed curves depict more skewed distributions of excitability where the majority of the granule cells are in a hypo-excitable state, which possibly resembles the excitability distribution in the adult DG. The two broader curves differ slightly in that one shows a more bimodal distribution.

Sources of immediate-early gene expression in the home cage remain unclear (Alme et al., 2010; Marrone, Schaner, McNaughton, Worley, & Barnes, 2008). Typically, home cage expression is treated as the negative gene expression control, which indicates basal levels of behaviorally-uncorrelated expression inherent across all conditions. It is, therefore, subtracted from the total observed behavioral expression to obtain a 'true' behaviorally relevant estimate of neuronal activity. The level of expression in the home cage, relative to behavior, in the present study was much higher than previously reported.

This may be reflective of methodological differences between studies, particularly in establishing microscope settings for image acquisition and determining threshold parameters for foci detection. Previous studies employed imaging and counting methods aimed at minimizing the appearance of home cage gene expression (e.g. Vazdarjanova & Guzowski, 2004); meanwhile, methods in the present study were somewhat on the opposite spectrum: the HV setting in the FITC channel was increased until foci in the home cage condition appeared just below saturation and detection thresholds were purposefully set low to be sensitive to and inclusive of small dim foci. Preliminary analysis of re-adjusting the threshold value to the mean of the home cage integrated intensity yielded much larger differences between home cage and behavioral expression (not shown here).

At least up to a point, integrated intensity of a focus is thought to directly relate to the amount of RNA transcripts present at the transcription site and may reflect the degree of recent activity - for instance, the number of laps run on a track (Miyashita, Kubik, Haghighi, Steward, & Guzowski, 2009). While the boolean method of analysis indicated no noticeable influence of behavior on DG gene expression, differences in foci characteristics between the caged controls and track runners indicate a clear behavioral effect (Figure 3.5A, 3.6A). Analysis of the foci across behavioral conditions showed significant increases in foci intensity in the track running groups relative to caged controls, across all hippocampal regions. Presumably, this reflects a significant increase in *H1a* mRNA transcription in the activated neurons as a result of electro-transcriptional coupling (Guzowski et al., 2006). In the DG and CA3, there were incremental increases

in integrated intensity going from the *HC* to *X1* to *X4* conditions, with CA3 foci exhibiting a significant difference between the small and large track (Figure 3.5B, 3.6B). This trend mirrors the increase in environment size, raising the possibility that the extent of gene expression in these subregions reflect environment-specific information such as the total area of exploration. Interestingly, in CA1 the integrated intensity difference between the *X1* and *X4* conditions was much smaller than in the other regions. It may be that CA3 and DG populations are more sensitive to changes in the environment, which has been suggested in some pattern separation studies (S. Leutgeb et al., 2004). In CA1, adults exhibited significantly bigger and brighter foci than juveniles, despite the juveniles running almost twice as many laps on the small track as on the large track (Figure 3.5C, 3.6C). The available data regarding the effect of lap number on foci size indicate a saturation of the effect after about 5 laps (Witharana, Clark, Trivedi, Lapointe, & McNaughton, 2012); thus, the observed difference between adult and juvenile foci in CA1 is more likely to be due to changes in electro-transcriptional coupling or changes in firing rate associated with development.

Conclusion

The preceding findings confirm previous observations that, in the adult DG, there is significant overlap in the active DG subpopulations across multiple environments. These data are consistent with the early retirement theory's hypothesis that a nonuniform distribution of excitability exists within the adult DG population in which relatively few neurons participate in many environments, while the vast majority of neurons exhibit

little to no activity in an environment. An activation probability near 0 was found in the juvenile DG, indicating that highly sparse, non-overlapping subpopulations participate in encoding events in a manner resembling random selection within a uniformly excitable population. Finally, the substantial difference in DG granule cell activation probability between juveniles and adults seems to support the hypothesis that postnatally generated, hyper-excitable neurons may contribute significantly to the excitable population within the GC layer.

Neurogenesis, however, is not the only mechanism by which the excitability of a neuronal population might become increasingly skewed over time. It would be beneficial for future studies to combine the present behavioral paradigm with a marker for recently born neurons in order to quantify their participation relative to mature neurons. This could be performed at additional age points between prepubescence and adulthood, and even in senescence, to obtain a useful profile of the changes in hippocampal activity patterns throughout life.

CHAPTER 5 BIBLIOGRAPHY

Alme, C. B., Buzzetti, R. A., Marrone, D. F., Leutgeb, J. K., Chawla, M. K., Schaner, M. J., . . . Barnes, C. A. (2010). Hippocampal granule cells opt for early retirement. *Hippocampus, 20*(10), 1109-1123. doi: 10.1002/hipo.20810

Altman, J. (1963). Autoradiographic Investigation of Cell Proliferation in Brains of Rats and Cats. *Anatomical Record, 145*(4), 573-&. doi: Doi 10.1002/Ar.1091450409

Altman, J., & Das, G. D. (1965). Autoradiographic and Histological Evidence of Postnatal Hippocampal Neurogenesis in Rats. *Journal of Comparative Neurology, 124*(3), 319. doi: Doi 10.1002/Cne.901240303

Bayer, S. A. (1982). Changes in the Total Number of Dentate Granule Cells in Juvenile and Adult-Rats - a Correlated Volumetric and H-3-Labeled 3-Thymidine Autoradiographic Study. *Experimental Brain Research, 46*(3), 315-323.

Bottai, D., Guzowski, J. F., Schwarz, M. K., Kang, S. H., Xiao, B., Lanahan, A., . . . Seeburg, P. H. (2002). Synaptic activity-induced conversion of intronic to exonic sequence in Homer 1 immediate early gene expression. *Journal of Neuroscience, 22*(1), 167-175. doi: 22/1/167 [pii]

Brakeman, P. R., Lanahan, A. A., O'Brien, R., Roche, K., Barnes, C. A., Huganir, R. L., & Worley, P. F. (1997). Homer: a protein that selectively binds metabotropic glutamate receptors. *Nature, 386*(6622), 284-288. doi: 10.1038/386284a0

Cameron, H. A., & McKay, R. D. G. (2001). Adult neurogenesis produces a large pool of new granule cells in the dentate gyrus. *Journal of Comparative Neurology, 435*(4), 406-417.

Chawla, M. K., Guzowski, J. F., Ramirez-Amaya, V., Lipa, P., Hoffman, K. L., Marriott, L. K., . . . Barnes, C. A. (2005). Sparse, environmentally selective expression of Arc RNA in the upper blade of the rodent fascia dentata by brief spatial experience. *Hippocampus, 15*(5), 579-586. doi: 10.1002/hipo.20091

Cole, A. J., Abu-Shakra, S., Saffen, D. W., Baraban, J. M., & Worley, P. F. (1990). Rapid rise in transcription factor mRNAs in rat brain after electroshock-induced seizures. *J Neurochem, 55*(6), 1920-1927.

Colgin, L. L., Leutgeb, S., Jezek, K., Leutgeb, J. K., Moser, E. I., McNaughton, B. L., & Moser, M. B. (2010). Attractor-map versus autoassociation based attractor dynamics in the hippocampal network. *J Neurophysiol, 104*(1), 35-50.

Epsztein, J., Brecht, M., & Lee, A. K. (2011). Intracellular determinants of hippocampal CA1 place and silent cell activity in a novel environment. *Neuron, 70*(1), 109-120.

Ge, S. Y., Yang, C. H., Hsu, K. S., Ming, G. L., & Song, H. J. (2007). A critical period for enhanced synaptic plasticity in newly generated neurons of the adult brain. *Neuron, 54*(4), 559-566. doi: Doi 10.1016/J.Neuron.2007.05.002

Gould, E., Beylin, A., Tanapat, P., Reeves, A., & Shors, T. J. (1999). Learning enhances adult neurogenesis in the hippocampal formation. *Nature Neuroscience, 2*(3), 260-265. doi: 10.1038/6365

Guzowski, J. F., McNaughton, B. L., Barnes, C. A., & Worley, P. F. (1999). Environment-specific expression of the immediate-early gene Arc in hippocampal neuronal ensembles. *Nature Neuroscience, 2*(12), 1120-1124. doi: 10.1038/16046

Guzowski, J. F., Knierim, J. J., & Moser, E. I. (2004). Ensemble dynamics of hippocampal regions CA3 and CA1. *Neuron, 44*(4), 581-584.

Guzowski, J. F., Miyashita, T., Chawla, M. K., Sanderson, J., Maes, L. I., Houston, F. P., . . . Barnes, C. A. (2006). Recent behavioral history modifies coupling between cell activity and Arc gene transcription in hippocampal CA1 neurons. *Proc Natl Acad Sci U S A, 103*(4), 1077-1082.

Hill, A. J. (1978). First occurrence of hippocampal spatial firing in a new environment. *Exp Neurol, 62*(2), 282-297. doi: 0014-4886(78)90058-4 [pii]

Jung, M. W., & McNaughton, B. L. (1993). Spatial Selectivity of Unit-Activity in the Hippocampal Granular Layer. *Hippocampus, 3*(2), 165-182.

Kato, A., Ozawa, F., Saitoh, Y., Hirai, K., & Inokuchi, K. (1997). vesl, a gene encoding VASP/Ena family related protein, is upregulated during seizure, long-term potentiation and synaptogenesis. *Febs Letters, 412*(1), 183-189.

Kee, N., Teixeira, C. M., Wang, A. H., & Frankland, P. W. (2007). Preferential incorporation of adult-generated granule cells into spatial memory networks in the dentate gyrus. *Nature Neuroscience, 10*(3), 355-362.

Kempermann, G. (2006). *Adult neurogenesis: stem cells and neuronal development in the adult brain*: Oxford University Press.

Kuhn, H. G., DickinsonAnson, H., & Gage, F. H. (1996). Neurogenesis in the dentate gyrus of the adult rat: Age-related decrease of neuronal progenitor proliferation. *Journal of Neuroscience, 16*(6), 2027-2033.

Leutgeb, S., Leutgeb, J. K., Treves, A., Moser, M. B., & Moser, E. I. (2004). Distinct ensemble codes in hippocampal areas CA3 and CA1. *Science, 305*(5688), 1295-1298.

Leutgeb, S., Leutgeb, J. K., Barnes, C. A., Moser, E. I., McNaughton, B. L., & Moser, M. B. (2005). Independent codes for spatial and episodic memory in hippocampal neuronal ensembles. *Science, 309*(5734), 619-623.

Leutgeb, J. K., Leutgeb, S., Moser, M. B., & Moser, E. I. (2007). Pattern separation in the dentate gyrus and CA3 of the hippocampus. *Science, 315*(5814), 961-966. doi: 10.1126/Science.1135801

Marr, D. (1971). Simple Memory - Theory for Archicortex. *Philosophical Transactions of the Royal Society of London Series B-Biological Sciences, 262*(841), 23-&. doi: 10.1098/Rstb.1971.0078

Marrone, D. F., Schaner, M. J., McNaughton, B. L., Worley, P. F., & Barnes, C. A. (2008). Immediate-early gene expression at rest recapitulates recent experience. *Journal of Neuroscience, 28*(5), 1030-1033.

Maurer, A. P., Cowen, S. L., Burke, S. N., Barnes, C. A., & McNaughton, B. L. (2006). Organization of hippocampal cell assemblies based on theta phase precession. *Hippocampus, 16*(9), 785-794. doi: 10.1002/hipo.20202

McNaughton, B. L., & Morris, R. G. M. (1987). Hippocampal Synaptic Enhancement and Information-Storage within a Distributed Memory System. *Trends in Neurosciences, 10*(10), 408-415.

Miyashita, T., Kubik, S., Haghighi, N., Steward, O., & Guzowski, J. F. (2009). Rapid activation of plasticity-associated gene transcription in hippocampal neurons provides a mechanism for encoding of one-trial experience. *Journal of Neuroscience, 29*(4), 898-906.

Muller, R. U., & Kubie, J. L. (1987). The effects of changes in the environment on the spatial firing of hippocampal complex-spike cells. *Journal of Neuroscience, 7*(7), 1951-1968.

O'Keefe, J., & Dostrovsky, J. (1971). The hippocampus as a spatial map. Preliminary evidence from unit activity in the freely-moving rat. *Brain Res, 34*(1), 171-175. doi: 0006-8993(71)90358-1 [pii]

Paxinos, G., & Watson, C. (2007). *The Rat Brain in Stereotaxic Coordinates* (6th ed.). Sydney, Australia: Academic Press.

Ramirez-Amaya, V., Marrone, D. F., Gage, F. H., Worley, P. F., & Barnes, C. A. (2006). Integration of new neurons into functional neural networks. *Journal of Neuroscience, 26*(47), 12237-12241.

Sala, C., Futai, K., Yamamoto, K., Worley, P. F., Hayashi, Y., & Sheng, M. (2003). Inhibition of dendritic spine morphogenesis and synaptic transmission by activity-inducible protein homer1a. *Journal of Neuroscience, 23*(15), 6327-6337.

Schlessinger, A. R., Cowan, W. M., & Gottlieb, D. I. (1975). Autoradiographic Study of Time of Origin and Pattern of Granule Cell-Migration in Dentate Gyrus of Rat. *Journal of Comparative Neurology, 159*(2), 149-175. doi: 10.1002/Cne.901590202

Schmidt-Hieber, C., Jonas, P., & Bischofberger, J. (2004). Enhanced synaptic plasticity in newly generated granule cells of the adult hippocampus. *Nature, 429*(6988), 184-187. doi: Doi 10.1038/Nature02553

Shiraishi-Yamaguchi, Y., & Furuichi, T. (2007). The Homer family proteins. *Genome Biology, 8*(2).

Stone, S. S. D., Teixeira, C. M., Zaslavsky, K., Wheeler, A. L., Martinez-Canabal, A., Wang, A. H., . . . Frankland, P. W. (2011). Functional convergence of developmentally and adult-generated granule cells in dentate gyrus circuits supporting hippocampus-dependent memory. *Hippocampus, 21*(12), 1348-1362.

Vazdarjanova, A., McNaughton, B. L., Barnes, C. A., Worley, P. F., & Guzowski, J. F. (2002). Experience-dependent coincident expression of the effector immediate-early genes arc and Homer 1a in hippocampal and neocortical neuronal networks. *Journal of Neuroscience, 22*(23), 10067-10071. doi: 22/23/10067 [pii]

Vazdarjanova, A., & Guzowski, J. F. (2004). Differences in hippocampal neuronal population responses to modifications of an environmental context: evidence for distinct, yet complementary, functions of CA3 and CA1 ensembles. *Journal of Neuroscience, 24*(29), 6489-6496.

Wilson, M. A., & McNaughton, B. L. (1993). Dynamics of the hippocampal ensemble code for space. *Science, 261*(5124), 1055-1058.

Witharana, W. K. L., Clark, B. J., Trivedi, V., Lapointe, V., & McNaughton, B. L. (2012). *Integrated fluorescence intensity of Homer1a transcription foci indicate integrated neuronal firing rates.* Poster presented at the Society for Neuroscience, New Orleans, LA, USA.

Xiao, B., Tu, J. C., & Worley, P. F. (2000). Homer: a link between neural activity and glutamate receptor function. *Current Opinion in Neurobiology, 10*(3), 370-374. doi: 10.1016/S0959-4388(00)00087-8

CHAPTER 6 APPENDIX

A. Supplementary Materials and Methods

Subjects. The adult animals were transported from the Charles River animal breeding facility at approximately 2.5 mo of age. The juvenile animals (post-natal day 28 on test day, P28) were bred at the Canadian Centre for Behavioral Neuroscience (CCBN) using breeding pairs that originated from Charles River animal facility. Adhering to CCBN animal protocol, rat pups were separated by sex and group weaned at P21 and placed into pair or triplet housing at P22.

Food reinforcement and restriction. During pre-training, animals were handled in the colony room for 5 min each and introduced to imitation chocolate sprinkles (Cake Mate® brand) in the home cage, twice daily for two days. The training period involved a morning and afternoon session for five days prior to test day. At the start of each morning training session animals were weighed, and any uneaten food pellets were removed from the home cage. At the end of each afternoon training session, 12-15 g per adult and 10-13 g per juvenile of dry food pellets were placed in each colony room cage overnight.

Long Evans pups typically experience tremendous weight gain during the time period coincident with the training period and testing. From post-natal day 21 to 29 (P21-P29), a male pup's weight is expected to double from around 50 g to 100 g, resulting in a weight gain of around 6 g per day (Charles River Research Models and Services 2012 Catalogue). Pups were given sufficient amounts of food to ensure normal weight gain.

Experiment room. The experiment room contained the two circular tracks, a table on which the animals rested in the holding boxes, and shelves containing various research-related equipment. The room lights were kept off, and a small lamp provided dim illumination.

Dark holding box. The semi-dark holding boxes (Figure 6.1) were constructed using clear plastic boxes, covered with opaque laminate material on the walls and lid, and drilled with air holes. A towel was placed at the bottom of the box for comfort.

Training. Training and testing occurred across months in six cohorts, each containing ten animals of the same age group. The training and testing for the last adult and last juvenile cohorts took place in a different room than that of the previous groups. However, the training apparatus and procedures remained consistent, and no obvious behavioral differences were noted from the location change.

On the first day, each rat freely explored the tracks and the connecting bridge for 10 min. For the next two days, animals learned to traverse between the tracks and run in the clockwise direction on each track. During days 4-5 of training, the connecting bridge was removed. While being carried from one track to the other by the experimenter, the animal was not covered and did not appear disoriented.

Figure 6.1 Pictures of the juvenile (left) and adult (right) dark holding boxes.

MECS settings. In the maximal electroconvulsive shock (MECS) treatment, a constant current passed through two points of contact on the head, in this case an electrode clip placed on each ear of the rat, to induce dramatic increase of early gene transcription (Cole et al., 1990; Guzowski et al., 1999). The ear electrodes were thinly lined by felt and soaked in 0.9% saline solution before attaching to the animal to decrease contact resistance. The constant-current generator used (Ugo Basile 57800) had the following settings: 100 pulses/sec, 0.5 msec pulse width, 1.1 sec shock duration, 85 mA current. MECS elicits a single, generally visible, seizure.

Perfusion-fixation. Each rat was anesthetized inside a 5% isoflurane container until no longer responsive (~40 sec); then, it was subcutaneously injected with sodium pentobarbital and transported to the perfusion room.

Animals were perfused on an ice bed to preserve the integrity of mRNA. 1X PBS and 4% PFA solutions were made from RNase-free, diethylpyrocarbonate (DEPC) treated water and maintained at ice-cold temperatures. PBS began at 28 min +/- 1 min.

Cryoprotection. Submersion in sucrose solution serves to cryoprotect the tissue from ice crystal damage when it is frozen (Carson, 1997). After submersion in 30% sucrose, the extracted hemispheres were frozen on crushed dry ice, wrapped in aluminum foil, and stored in plastic containers at -80 ^{o}C until sectioning.

Tissue blocking and sectioning. Superfrost-plus slides were lightly wetted with 1X PBS made with DEPC-treated water. Precise adjustments to unfold tissue or smooth away trapped air bubbles were performed using small paintbrushes that were treated with RNAse Away. Slides were dried at room temperature, frozen at -20 ^{o}C overnight, and subsequently stored at -80 ^{o}C.

FISH. Riboprobes targeting the 3' UTR of the *Homer1a* gene were created from *H1a* DNA using a transcription synthesis kit (Maxscript; Ambion). Target mRNA transcripts were fixed in place using buffered 4% PFA and washed in 2X saline sodium

citrate (SSC) buffer. To increase access of the probe to target transcripts, slides were incubated with 0.3% proteinase K buffer, fixed with 4% PFA, treated with 0.5% acetic anhydride, incubated in 1:1 methanol and acetone solution, and washed in 2X SSC. Slides were incubated with 150 µl each of prehybridization buffer for 1 h in a 2X SSC/ formamide humid chamber at room temperature. Immediately following, slides were coverslipped and incubated in a humid chamber for 16 hr at 56 °C.

Slides were removed from the oven to allow to cool for 15 min. RNase A (10 mg/ ml) at 37 °C was used to degrade any single-strand RNA for 30 min. Slides were washed with 2X SSC, then 0.5X SSC at 55 °C for 30 min. After quenching endogenous peroxidases in 2% H_2O_2 for 15 min, slides were blocked with blocking buffer + 5% sheep serum for 1 h at room temperature and incubated with 1:1000 anti-fluorescein in blocking buffer in a humid chamber at 4 °C overnight.

Slides were washed with Tris-buffered saline containing 0.05% Tween-20 and incubated with 1:100 FITC-tyramide dye (Perkin Elmer) for 30 min. Slides were washed in TBS buffer and counter-stained with 1:1500 DAPI in TBS (Sigma). DAPI (4'-6-diamidino-2-phenylindole) nucleic acid stains target DNA in cell nuclei, which serves as a useful tool for co-localizing apparent *H1a* foci with a neuron. Following washing in TBS, slides were coverslipped using a small amount of Vectashield (Vector Labs), allowed to dry for 1-2 days at 4 °C, and sealed with nail polish.

Sampled coordinates along the coronal axis. The sections used in foci quantification were from the right hemisphere of the dorsal hippocampus (Bregma -3.00 to -4.00 mm) (Figure 6.2).

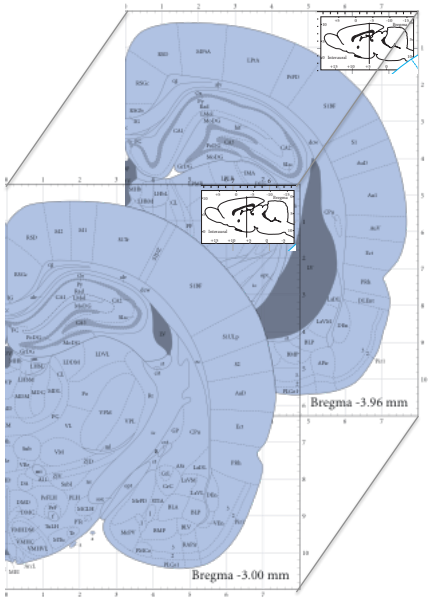

Figure 6.2 Brain atlas depiction of range of sampled positions along the coronal axis. Modified from The Rat Brain Atlas (Paxinos & Watson, 2007).

Image acquisition parameters. Table 6.1 lists the parameters values employed during image acquisition on the confocal microscope for all image stacks.

Table 6.1 Confocal acquisition parameters used for image stacks.

Image Acquisition Parameter	Parameter Value
Scan mode	Oneway
Scan speed	2.0 µs/pixel
Pixel resolution	1024 by 1024
Zoom	1.0
Objective lens	40X oil immersion
Laser output	DAPI Channel 5% FITC Channel 5%
HV	DAPI Channel varied by section FITC Channel varied by slide
Gain	0
Offset	0%
Confocal aperture	70 µm
Step-size	1 µm

IEG Analysis user-specified thresholds. The IEG Analysis software for automated foci detection was developed by Vivek Trivedi in the McNaughton laboratory. Table 6.2 lists the user-specified parameter values used for foci detection across all image stacks.

Table 6.2 User-specified thresholds in IEG Analysis software used for foci detection.

Threshold Parameter	Threshold Value
Minimum Blue Intensity	25
Minimum Blue %	50
Minimum Green Intensity	25
Minimum Peak Green Intensity	60
Minimum Green Blob Volume (pixels)	20
Minimum z layers required for blob	2

IEG Analysis software output. Table 6.3 lists the output headings from the IEG Analysis software for the intranuclear foci identified in an image stack, and provides a brief description of the heading.

Table 6.3 Output categories in IEG Analysis software.

Result Field	Description
Image Title	Name of the image
INF No.	INF ID to identify the particular INF object
CenterX	Spatial X coordinate of INF's maxima
CenterY	Spatial Y coordinate of INF's maxima
CenterZ	Spatial Z coordinate of INF's maxima
Volume	Total number of pixels in INF object
AreaXY	Area in XY plane
AreaYZ	Area in YZ plane
AreaXZ	Area in XZ plane
Mean Intensity	Average intensity of INF
Background	Default background
Max Intensity	Maximum intensity
Min Intensity	Minimum intensity
Range	Max Intensity minus Min Intensity
Intensity Integral	$\sum_{i=0}^{n} P_i$, P_i is the intensity value of the ith pixel
Saturated Pixels	Number of pixels with $P_i = 255$
% Saturation	Percentage of saturation in the INF; number of saturated pixels over total number of pixels*100

Normalizing foci count by volume. The region sampled in each image stack was restricted to only the molecular layer of the upper blade of the DG, the CA3, and CA1. The region of interest was outlined freehand using ImageJ. The number of pixels within the ROI was converted to an area, based on the relationship of 3.226 pixels:1 μm, and multiplied by the thickness of the section (the number of z-layers at 1 μm step-size) to arrive at the volumetric estimate.

This method for normalization is useful for comparing normalized foci counts for the same brain region, since it assumes that a similar number of neurons are sampled due to similarly packed cells. However, it is limited for comparing across brain regions, such as across the subregions of the hippocampus or various cortical regions where cell densities differ. It does provide information consistent with normalizing by the sum of blue pixels in the ROI (which appears the best option; comparison not shown here).

Normalizing foci counts by the number of blue channel pixels is particularly useful when analyzing between different brain regions (in which density of cell packing may vary) and comparing across sections (in which the sampled volume may vary due to section thickness or position along the sampled axis).

Normalizing foci count by MECS. Figures 6.3A-C and 6.4A-C show the proportion of *H1a* positive neurons with respect to experience and age in the DG, CA3, and CA1 regions. The foci count from each behavioral condition was normalized by the positive gene expression control, a.k.a. MECS, foci count to produce an estimate of the proportion of active cells.

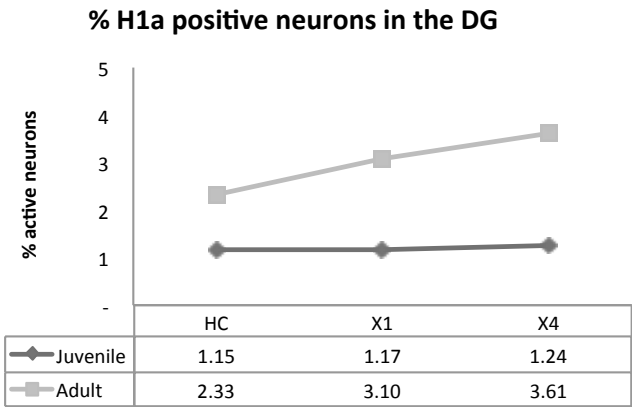

Figure 6.3A Proportion of *H1a* positive neurons with respect to experience and age in the DG. The foci count from each behavioral condition was normalized by the MECS foci count to produce an estimate of the proportion of active cells.

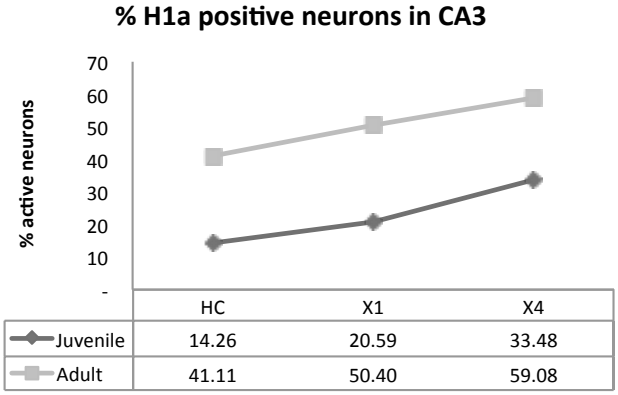

Figure 6.3B Proportion of *H1a* positive neurons with respect to experience and age in CA3.

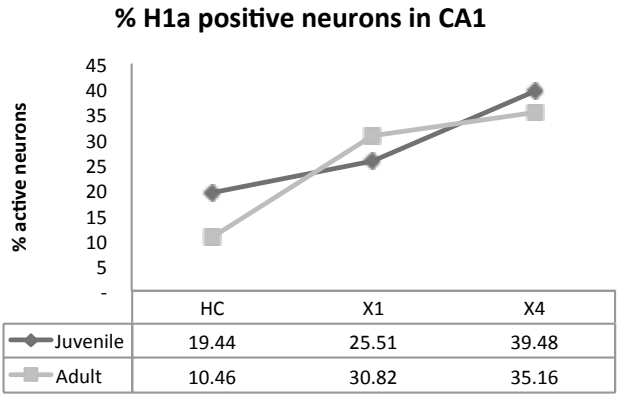

Figure 6.3C Proportion of *H1a* positive neurons with respect to experience and age in CA1.

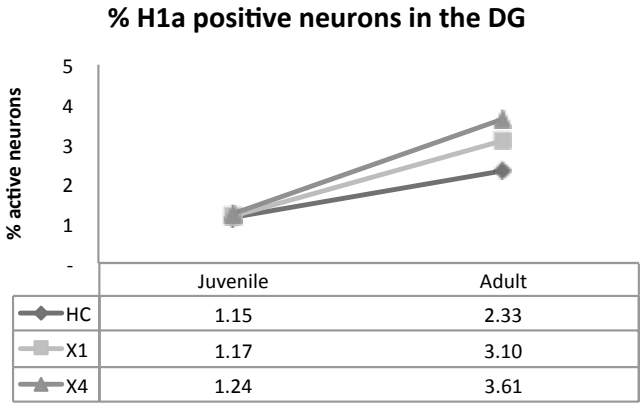

	Juvenile	Adult
HC	1.15	2.33
X1	1.17	3.10
X4	1.24	3.61

Figure 6.4A Proportion of *H1a* positive neurons with respect to experience and age in the DG. Graphically presents the same data as Figures 6.3A on switched axes.

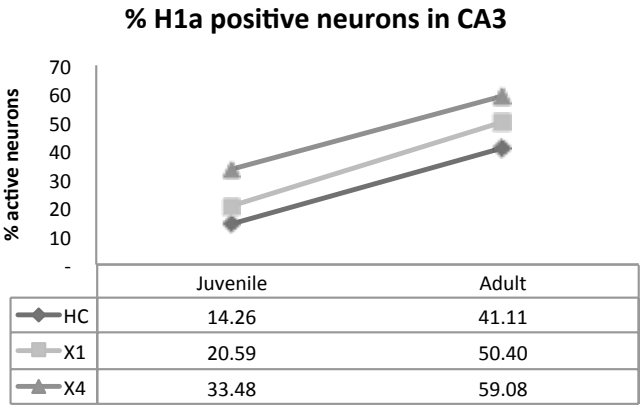

	Juvenile	Adult
HC	14.26	41.11
X1	20.59	50.40
X4	33.48	59.08

Figure 6.4B Proportion of *H1a* positive neurons with respect to experience and age in CA3. Graphically presents the same data as Figures 6.3B on switched axes.

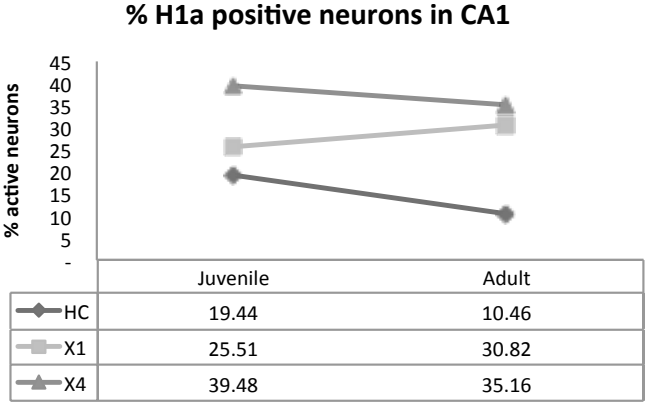

	Juvenile	Adult
HC	19.44	10.46
X1	25.51	30.82
X4	39.48	35.16

Figure 6.4C Proportion of *H1a* positive neurons with respect to experience and age in CA1. Graphically presents the same data as Figures 6.3C on switched axes.